



Article

Efficient (Bio)emulsification/Degradation of Crude Oil Using Cellulose Nanocrystals

Petr Sitnikov ¹, Philipp Legki ¹, Mikhail Torlopov ¹, Yulia Druz ¹, Vasily Mikhaylov ¹, Dmitriy Tarabukin ², Irina Vaseneva ¹, Maria Markarova ^{2,3}, Nikita Ushakov ¹ and Elena Udoratina ^{1,*}

¹ Institute of Chemistry, Komi Science Centre, Ural Branch of the Russian Academy of Sciences, Pervomayskaya Str. 48, Syktyvkar 167000, Russia; sitnikov-pa@mail.ru (P.S.); philipp2374372@mail.ru (P.L.); tanlan799@gmail.com (M.T.); yuliadruz@gmail.com (Y.D.); system14@rambler.ru (V.M.); ir_vaseneva@mail.ru (I.V.)

² Institute of Biology, Komi Science Centre, Ural Branch of the Russian Academy of Sciences, Kommunisticheskaya Str. 28, Syktyvkar 167982, Russia; dim1822@yandex.ru (D.T.)

³ Federal Scientific Vegetable Center, Selectionnaya Str. 14, VNISSOK, Odintsovo District, Moscow 143072, Russia

* Correspondence: udoratina-ev@chemi.komisc.ru

Abstract: This study has investigated the influence of cellulose nanocrystals (CNCs) with partially acetylated surfaces on the formation, stability, rheology and biodegradability of the Pickering emulsion in a crude oil/water (co/w) system. In all investigated systems, it was observed that the CNC concentrations of 7 mg/mL led to the emulsions showing stability over time. It was also noticed that the increase in concentration of background electrolyte (NaCl) leads to the droplets of emulsions becoming smaller. It was demonstrated that the rheology of the o/w emulsions of the oil products and crude oil stabilized by CNCs depends, to a large extent, on the colloid chemical properties of nanocellulose particles. Calculations and experimental methods were used to study the changes in the acid–base properties of CNCs on the surface of emulsion droplets, depending on a type of hydrophobic components (crude oil and liquid paraffin). The formation of Pickering emulsions leads to the oxidation of oil by *Rhodococcus egvi* in aerobic conditions becoming more effective, provided that the environment includes mineral salts of nitrogen, potassium and phosphorus. The results obtained present a scientific basis for the development of technologies for the disposal of oil spills on water surfaces.

Keywords: Pickering emulsion; cellulose nanocrystals; oil biodegradation; crude oil



Citation: Sitnikov, P.; Legki, P.; Torlopov, M.; Druz, Y.; Mikhaylov, V.; Tarabukin, D.; Vaseneva, I.; Markarova, M.; Ushakov, N.; Udoratina, E. Efficient (Bio)emulsification/Degradation of Crude Oil Using Cellulose Nanocrystals. *Polysaccharides* **2023**, *4*, 402–420. <https://doi.org/10.3390/polysaccharides4040024>

Academic Editor: Florin Oancea

Received: 30 June 2023

Revised: 12 October 2023

Accepted: 19 October 2023

Published: 10 November 2023



Copyright: © 2023 by the authors. Licensee MDPI, Basel, Switzerland. This article is an open access article distributed under the terms and conditions of the Creative Commons Attribution (CC BY) license (<https://creativecommons.org/licenses/by/4.0/>).

1. Introduction

Over the last decade, while the development of nanotechnologies allowed for the generation of highly dispersed particles in an amount sufficient to satisfy the needs of industry, the number of studies of Pickering emulsions has been rising steadily. This type of dispersed system is an alternative to traditional surface-active agents (surfactants) and consists of small liquid droplets (with the diameter between 0.5 and 10 µm, as a rule) distributed in a dispersing medium and stabilized by solid particles. Pickering emulsions are widely used in the food, cosmetics, medical and oil refining industries [1].

Studies have been conducted on the stabilization of oil/water emulsions by non-organic particles: aerosol [2], layered minerals [3,4], graphene oxide [5], etc. In recent years, there has been a significant trend towards green materials based on nanostructured derivatives of polysaccharides—cellulose and chitin [6,7]. Due to their high biodegradability, these “green” materials compare favorably with the traditional synthetic surfactants, which are toxic to various components of ecosystems.

Cellulose nanocrystals (CNCs) feature a set of unique properties: a highly organized structure and large surface area, low density, increased chemical stability and a comparatively broad range of possibilities for surface modification in combination with high

mechanical properties. As a rule, CNC is generated using acid hydrolysis of vegetation biomass [8].

In order to form stable emulsions, a particle should exhibit good wettability of both hydrophilic and hydrophobic components. Kalashnikova et al. [9] show that the faces of CNCs are structurally non-equivalent, and the amphiphilicity of I α and I β cellulose is based on (200) β /(220) α -hydrophobic edge plane. The following factors which influence the formation and stability of nanocellulose-based Pickering emulsions can be distinguished: the geometry of nanoparticles, the chemical nature of the surface and its charge, the ionic strength and the pH of a dispersed medium [10–12]. Water dispersions of CNCs have a negative surface charge due to the orientation of dipoles in the dispersed medium, the dissociation of electrolytically active groups and other factors [13]. Although sulfuric acid hydrolysis is one of the commonly used methods of CNC particle generation, the sulfated CNCs cannot effectively stabilize oil droplets due to the strong repulsion between nanoparticles, which inhibits their adsorption on the oil/water interface. Research has shown that sulfated CNCs with a surface charge exceeding -50 mW cannot effectively stabilize oil droplets because of strong electrostatic repulsion between the nanoparticles in the area of the oil/water interface [9]. Additional treatment of CNC—that is, removal of sulfate groups from the surfaces of nanocrystals—leads to a reduction in the surface charge to -35 mW, which has a favorable effect on their emulsifying ability. Recently, there have also been methods developed for the direct extraction of CNCs with a composition and nanocrystal properties that are more suitable for these purposes [14].

The issues of the formation of CNC-stabilized Pickering emulsions in oil/water systems have been studied in detail for various simulated and natural hydrophobic compounds: hexadecane, styrene [6,15], dodecane [13], palm oil [16], etc. However, there has been little research on the formation of the mentioned colloid dispersions in the crude oil/water (co/w) systems. At the moment, the problems arising in connection with the formation of emulsions in oil-containing systems are mainly related to the separation of water from crude oil [17]. The authors of [17–21] point out that in such cases, this activity is complicated due to the presence of natural emulsifiers (fatty acids, asphaltenes), as well as highly dispersed mineral particles (argillites, quartz etc.) capable of generating their own Pickering emulsions [22].

Due to their dual hydrophilic/hydrophobic nature and non-toxicity, CNCs have great potential as a “green” emulsifier, stabilizer and gelling agent for prospective biotechnologies that are applied in the elimination of crude oil spills without secondary environmental damage. One of the ways to expedite the removal of oil contamination is to make use of hydrocarbon-oxidizing microorganisms able to produce and release into the environment natural surface-active agents, namely, biosurfactants [23–27], which interact with oil products that are hydrophobic in nature and intensify their biodegradation in the soil [28]. In particular, Parajuli et al. [29] showed that *Serratia marcescens* stock can effectively process saturated hydrocarbons in Pickering emulsions in co/w systems stabilized by sulfated CNCs.

In this study, we aimed to develop eco-friendly oil emulsifiers based on CNCs and to assess the effectiveness of oil emulsion biodegradation after the introduction of target oil-destroying microorganisms. For this, we have studied the influence of CNCs with partially acetylated surfaces on the formation and stability of Pickering emulsions in a crude oil/water system depending on component ratio, ionic strength and pH of the medium, and we have examined the biodestruction of the obtained emulsions by natural microorganisms.

2. Materials and Methods

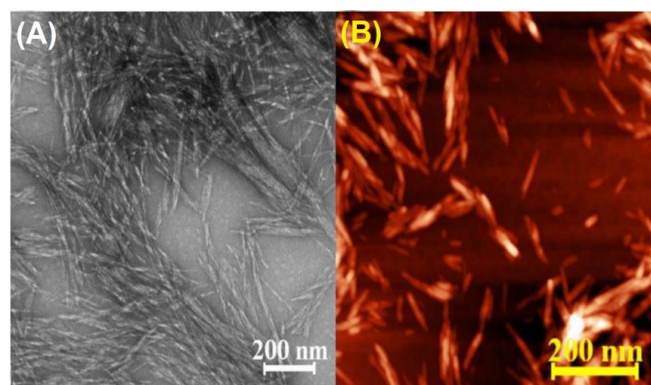
2.1. Materials

Crude oil (Usinsk, Russia) was used in the study. The general characteristics of the Russian Urals oil, as determined by the laboratory of the refinery company, are summarized in Table 1.

Table 1. General characteristics of crude oil.

Parameter	Value
Density at 20 °C (kg/m ³)	877.5
Water (wt.%)	0.09
Mass concentrations of chloride salts (mg/dm ³)	22.1
Sulfur (wt.%)	1.24
Mechanical impurities (wt.%)	0.0092
Paraffin (wt.%)	7.2
Resins (wt.%)	15.66
Asphaltenes (wt.%)	3.81
Crystallization temperature (°C)	+7
Mass fraction of organic chlorides (ppm)	<1
Mass fraction of hydrogen sulfide (ppm)	9.7
Mass fraction of methyl-ethyl mercaptan (ppm)	6.2

CNCs, as a hydrosol, were used as a stabilizer for o/w emulsions. CNC was obtained by the previously proposed method of controlled solvolysis of cellulose in acetic acid/1-Octanol in the presence of hydrogen peroxide and phosphotungstic acid. The isolation, purification and characterization of CNCs are described in detail by Torlopov et al. [30]. Dispersing phase concentration in the prepared hydrosol was determined using the gravimetric method. As a result of solvolysis under these conditions, CNC with a partially acetylated surface has been obtained. The content of acetic surface groups amounted to 13.5 per 100 anhydroglucose units. Microscopic analyses data (Figure 1) support the rod-like morphology of particles with average geometric dimensions of approximately 200 nm (length) and 8 nm (width, thickness). The ζ -potential of cellulose nanoparticles in aqueous solution is about -35 mV. The supramolecular structure of CNC corresponds to the first type of cellulose allomorphs, and the crystallinity index is 0.88.

**Figure 1.** Morphology and sizes of CNCs used as dispersant: TEM (A) and AFM (B) images.

2.2. Emulsion Preparation

The co/w emulsions were prepared using crude oil and a CNC aqueous suspension at the required concentration without dilution. All the emulsions were prepared using an oil/aqueous phase ratio of 30:70. Basically, 0.3 mL of crude oil was added to 0.7 mL of aqueous suspension in a glass vial and sonicated with an ultrasonic device IL 10 (Russia) with a dipping titanium probe close to the surface (power corresponds to 2 V/mL applied power determined by Cavitometr ICA-5D) for 20 s. In order to determine the optimum mass ratio of CNCs and oil, the ratio was varied by diluting the water dispersion of CNC while maintaining a fixed value of background electrolyte concentrations.

2.3. Rheological Behavior of Emulsions

Rheological and flow profiles of o/w emulsions were obtained with a Brookfield DV-III+ Ultra rheometer (Brookfield Engineering Laboratories Inc., Middleboro, MA, USA)

manned with an adapter for small amounts. Before measurement, a sample was thermostated for 25 min. Measurements were taken at a temperature of 25 ± 0.1 °C. The duration of measurements at each point was 20 s. Shear viscosity was measured at a shear rate ranging from 5 to 264 s^{-1} .

To analyze the experimental data of rheological curves in shear rate vs. shear stress coordinates, two models were used.

Bingham model (Equation (1)) [31]:

$$\tau^B = \tau_0^B + \mu_p^B \dot{\gamma} \quad (1)$$

where τ_0^B mPa—Bingham yield stress; μ_p^B —the plastic viscosity; mPa·s, $\dot{\gamma}$ —the shear rate, s^{-1} .

The apparent viscosity (μ_a^B) at a certain value of shear stress was calculated via Equation (2):

$$\mu_a^B = \mu_p + \frac{\tau_0}{\dot{\gamma}} \quad (2)$$

The parameters τ_0 and μ_p denote the rheological curves and the apparent viscosities. Power law model, Equation (3) [32]:

$$\tau = K \dot{\gamma}^n \quad (3)$$

where K and n are the rheological parameters, known as the consistency index and the flow behavior index. The apparent viscosity (μ_a^{pl}) was calculated via Equation (4):

$$\mu_a^{pl} = K \dot{\gamma}^{n-1} \quad (4)$$

2.4. Acid–Base Properties of o/w Emulsion

The protonation/deprotonation processes on the surfaces of the CNCs at the time of the formation of an emulsion were varied by potentiometric acid–base titration using the automatic titrator Aquilon ATP-02 (company “Akvilon”, Podolsk, Russia). The sample volume was 50 mL, and the weight of CNCs was 0.375 g. The temperature of the titrated solution in the thermostated cell was 25 °C and kept constant with an accuracy of 0.25 °C. The solution was stirred with a magnetic stirrer. The pH values were measured after the addition of each titrant portion and only after the equilibrium was established (after 15–20 min). The titration was conducted in an argon atmosphere in polypropylene vessels with constant concentrations of background electrolyte (NaCl, 0.001, 0.01, 0.1 M). Every sample was titrated three times. In order to interpret the titration curves, this work made use of 2pK-approximation within the framework of the double electrical layer theory. Acid–base processes on the surface of the particles were described using the simulation model given in the paper [33], which permits the calculation of the surface complexation constants (pK_i) of related adsorption surface centers according to their ability to convert into acid (pK_2) or base (pK_1) forms depending on the pH of the medium, taking into account the sorption of cations (pK_M) and anions (pK_A) of the background electrolyte. This approach also permits us to determine the concentration of the related surface acid–base centers in a compound with an unknown chemical composition. Titration was conducted using 0.01 M solution of NaOH; therefore, the surface complexation values were calculated for pK_M and pK_2 .

Based on these findings, the proton Gibbs adsorption (n_b , mmol/g) depending on pH of the medium, was calculated via the following Equation (5):

$$n_b = (V_{total} \times (C_0 - C_e)) / m_{Cell}, \quad (5)$$

where V_{total} is the volume of the titrated system; $C_0 - C_e$ is the difference between the added concentration (C_0) of the potential determining ion (H^+ , OH^-) and the concentration measured with pH meter (C_e); and m_{Cell} is the mass of cellulose in the system.

The acid–base properties of the CNCs on the surface of the emulsion droplets varied depending on the type of hydrophobic component using a simulated compound—liquid paraffin—with density values close to those of crude oil (0.880 and 0.877 g/mL, respectively). Liquid paraffin is a mixture of saturated hydrocarbons C₁₁–C₁₅, which allows for the exclusion of the interference of polar oil molecules during the formation of the emulsion.

2.5. Optical Light Microscopy

The optical light microscopy of the emulsions was conducted using an Olympus BX53 optical microscope with UCMOS14000KPA camera (ToupTek, Hangzhou, China) and ToupView software (version 3.7). The microscope uses 100× lenses. Both direct microscope inspection and a fluorescent one with a green filter (520–560 nm) were used, as oil fluoresces well within the abovementioned wavelength range due to aromatic hydrocarbons. Particle size was analyzed using ImageJ software (version 1.52 u).

2.6. Transmission Electron Microscopy (TEM)

TEM was used to study CNC morphology (Tecnai G2 spirit Biotwin, FEI, Portland, OR, USA) with an acceleration tension of 100 kV. A drop of diluted CNC suspension (0.03%) was deposited onto a copper grid covered by a thin carbon film and then analyzed after drying at ambient temperature.

2.7. Atomic Force Microscopy (AFM)

For AFM, a Solver P47 (state corporation NT-MDT, Saint Petersburg, Russia) in the semi-contact mode was used with HA-HR probes (NT-MDT, ETALON series). A drop of the suspension (10 µL) was placed onto a freshly cleaved mica surface, incubated for 5 min and dried by air flow.

2.8. Biodegradability of Crude Oil and co/w Emulsions

The biodegradability of crude oil and co/w emulsions was studied in a phosphate buffer (0.01 M, pH 6.8) in order to ensure an optimum ratio of microelements (10% mass ammonium nitrogen and 25% mass total phosphates, calculated with reference to P₂O₅, 25% mass potassium, calculated with reference to K₂O). The experiment duration was 30 days. The temperature was 21 ± 1 °C. In the experiment, we used co/w emulsions with a CNC content of 7 mg/mL in the absence of an electrolyte.

2.9. Microbial Inoculums Preparation

The inoculum of microorganisms was a culture of hydrocarbon-oxidizing coryneform bacteria *Rhodococcus egui*. The culture was isolated from the oil-contaminated soil in the area of the oil spill accident in the Usinsk district of the Komi Republic. The biomass was generated during liquid-phase fermentation in a semi-synthetic medium and dried via spray dehydration. The dry cell titer is (10⁶/g) 3.5–4.8 × 10⁹. A standard solution of hydrocarbon-oxidizing culture was prepared by diluting dry cells by 10⁴ with water (0.12 g per 1000 mL of water). For each version of the bioproduct, 1 cm³ of the standard solution of microbial suspension was used.

2.10. Assessment of Residual Total Petroleum Hydrocarbons (TPH) Content

The TPH content in the soil samples has been determined using the gravimetric method [34]. The identification of n-alkanes was conducted using a KRISTALL 5000 gas chromatograph (Chromatek, Yoshkar-Ola, Russia) with a flame ionization detector in the column thermostat temperature programming mode (130 °C–8 °C/min–360 °C) in the quartz capillary column with dimensions of 30 m × 0.25 mm (HP-5MS), as well as liquid stationary phase phenyl polysiloxane (5%) and a film thickness of 0.25 µm. The carrier gas was 99.99% helium. The inlet pressure of the carrier gas was 100 kPa, and the split ratio was 1:50. Auxiliary gas flow rates: hydrogen—20 mL/min; air—200 mL/min. The evaporator temperature was 300 °C, and the detector temperature was 250 °C. The sample

containing oil products was diluted in 0.5 mL of toluene (extra pure grade) containing internal standard (decane).

3. Results and Discussion

3.1. Conditions for Formation and Stability of Emulsions

To study the conditions in which emulsions are formed, the following parameters were varied: the ratio of initial components; concentrations of NaCl in the volume; the pH of the sub-system being studied. Figure 2 shows microphotographs of emulsion droplets in the co/w system depending on the mass fraction of CNCs and the concentration of the background electrolyte. The change in sizes of emulsion droplets is demonstrated in Figure 3.

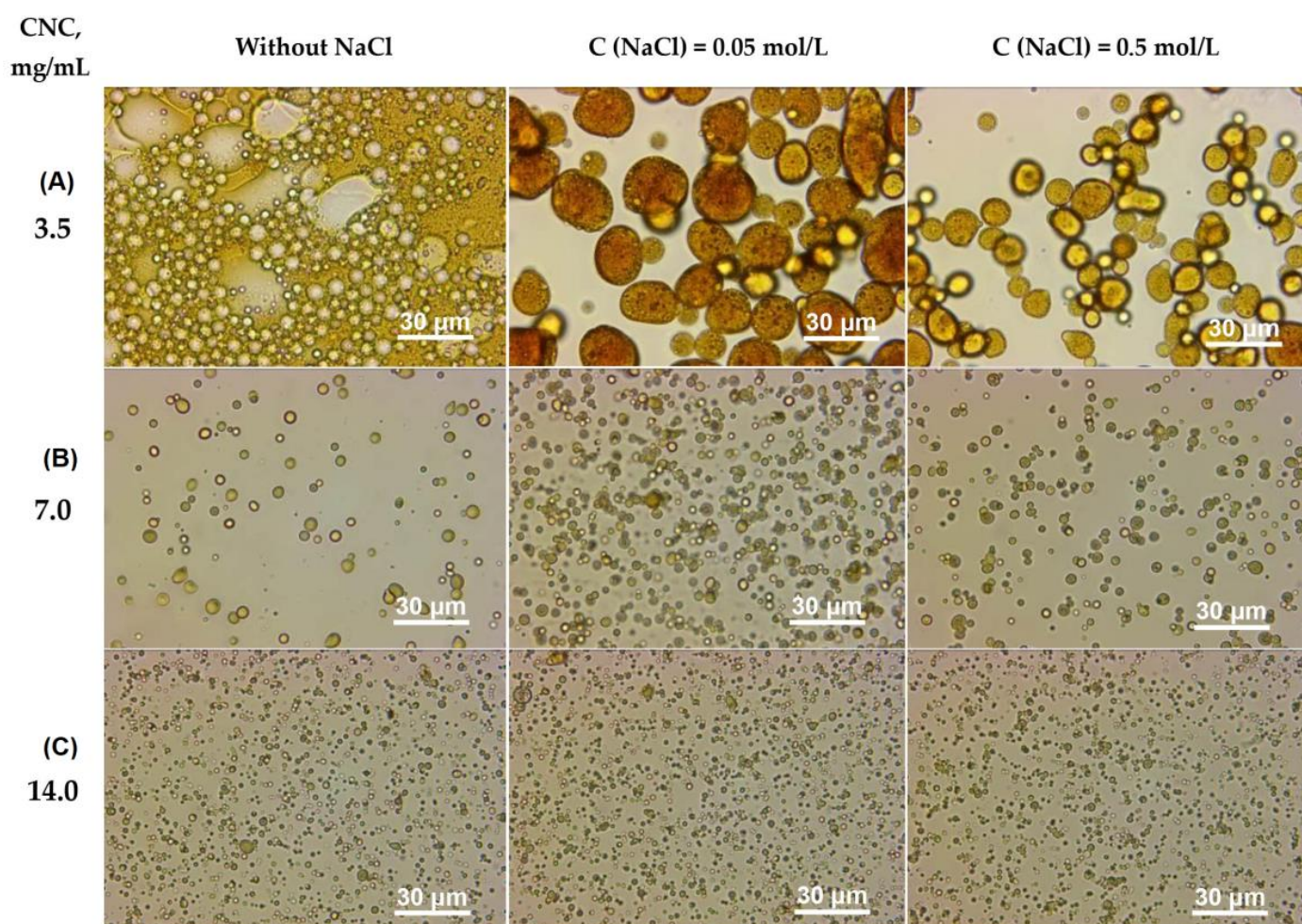


Figure 2. Microphotographs of emulsion droplets in the co/w system based on the optical microscopy data, depending on CNC content: (A) 3.5; (B) 7; (C) 14 mg/mL.

In oil/water emulsions containing CNCs in the amount of 3.5 mg/mL, it can be observed that the inversion of emulsions begins if the background electrolyte is absent (Figure 2A). This relates to asphaltenes, the emulsifiers present in oil (Table 1). An increase in the concentration of NaCl leads to the transition to formation of co/w Pickering emulsions (at $C(\text{NaCl}) \leq 0.05 \text{ M}$). Kalashnikova et al. [6] and Capron et al. [15] showed that the cations of background electrolyte become involved in the building of a 2D network out of nanocrystals on the surface of the emulsion droplets. It should be noted that with the increase in cation quantity, a decrease in electrostatic repulsion between negatively charged nanocrystals is observed, which leads to a shortening of the distance between particles. This can be considered as a reason why the sizes of emulsion droplets decrease in a co/w

system with an increase in the concentrations of background electrolyte (Figure 3). The increase in the mass fraction of CNCs in the system (Figure 3B,C) leads to a decrease in the sizes of emulsion droplets due to the formation of closer-packed 2D structures. In co/w systems with nanocrystal content mounting to 7 mg/mL, the average size of droplets is 3 μm , and if CNC content becomes as high as 14 mg/mL, their size decreases to 1.5 μm . Any further increase in CNC concentrations does not cause a significant decrease in sizes of emulsions droplets. The use of CNCs with partially acetylated surfaces, unlike their sulfated forms [29], allowed for a 10-times decrease in the size of oil droplets, i.e., from 20 μm to 1.5 μm . This result can be explained by the formation of a network of native nanocrystals of cellulose on the oil surface in a closer-packed array due to the weakening of the electrostatically repulsive forces in comparison with sulfated CNCs (S-CNC) (ξ -potential of n-CNC is -35 mV, and ξ -potential of S-CNC is -50 mV) [30].

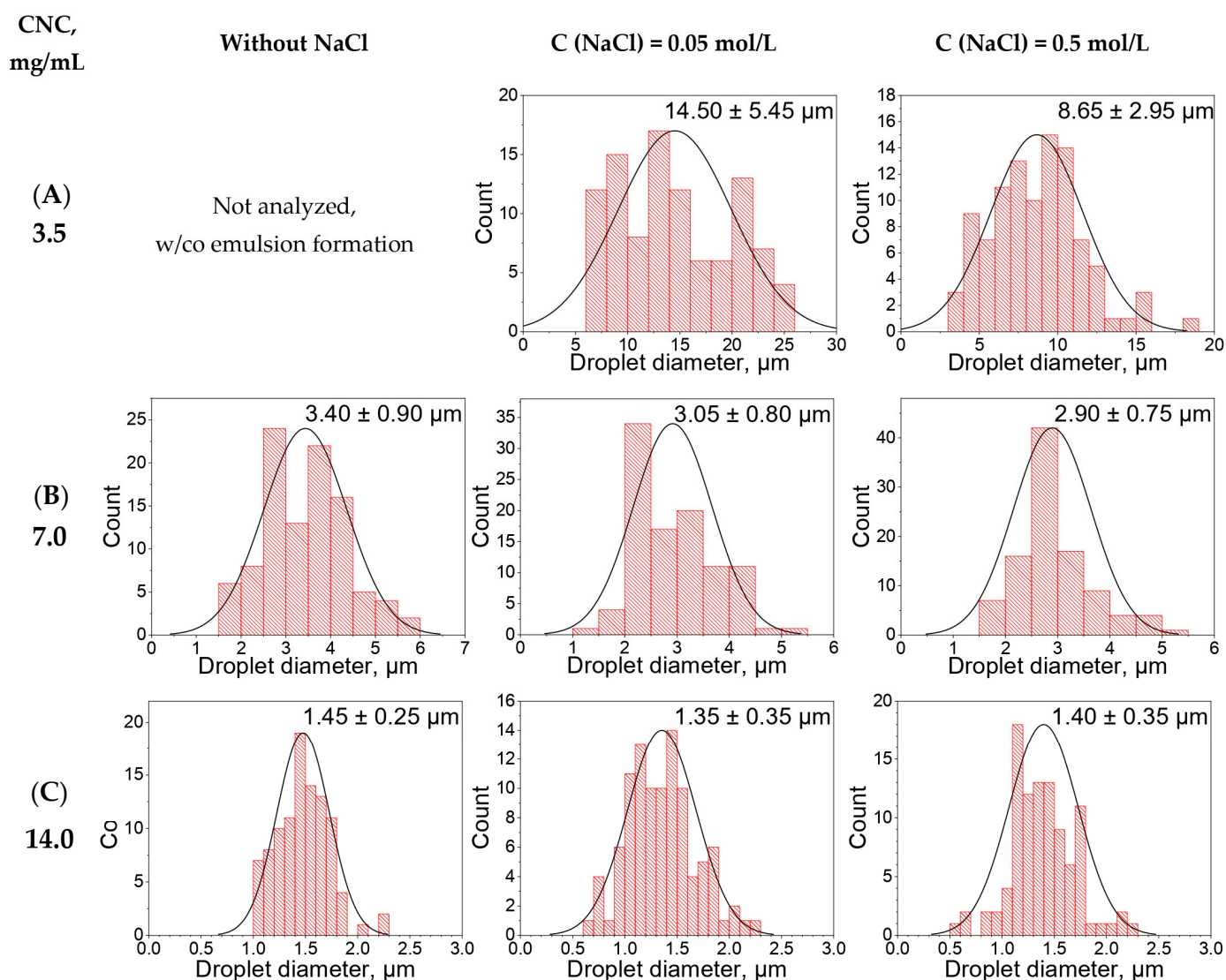


Figure 3. Distribution histograms of emulsion droplets in the co/w system based on the optical microscopy data, depending on CNC content: (A) 3.5; (B) 7; (C) 14 mg/mL.

In all the studied systems, once cellulose concentrations become higher than 7 mg/mL, the formation of kinetically stable emulsions is observed. Therefore, the experiments aiming to investigate the acid–base properties have made use of systems with the CNC concentration of 7 mg/mL, as this is the minimum and sufficient concentration of CNCs required for the formation of emulsions that are stable over time.

In the natural environment, the formation and stability of emulsions can be influenced by the pH of the environment. For instance, in the Arctic territories, due to the slow deterioration of organics, water reservoirs contain a large amount of humic and phenolic acids which cause the acidification of those reservoirs. Figure 4 shows changes in the structure of emulsions in relation to ambient pH.

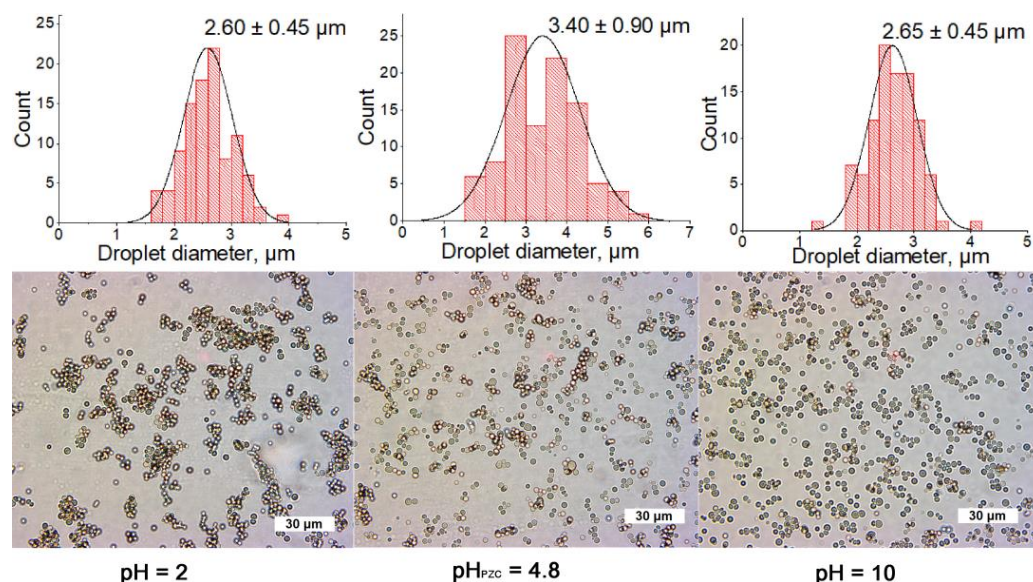


Figure 4. Micrographs of CNC-stabilized co/w emulsions at various pH values according to the data obtained via optical microscopy (emulsion cure time is 120 min).

The change in the pH of the emulsion is accompanied by a decrease in the average size of emulsion droplets (Figure 4), which may be accounted for by the aforementioned electrolytic effect. In view of that effect, in the case of an increase in pH, the cations of the added alkali (0.1 M NaOH) neutralize the surface charge of CNC, thus allowing for the formation of a more uniform and closer-packed 2D surface structure. In the case of a decrease in pH (0.1 M HCl), the protons of the strong acid act to suppress the dissociation of the surface acid–base centers (of carboxyl and hydroxyl groups), which results in the agglomeration of emulsion droplets. As is shown in Figure 4, variations in pH significantly impact the morphological parameters and the geometry of microdroplets of CNC-based Pickering emulsions. Hence, the formation of such systems is immensely influenced by acid–base interactions.

3.2. Study of Acid–Base Properties of Emulsions

Figure 5 presents the data concerning the fluctuations in proton adsorption (n_b) in aqueous dispersions of CNC, Pickering emulsions containing crude oil and liquid paraffin, depending on pH and the concentrations of the background electrolyte.

All emulsions are stable within the pH range from 3.5 to 7.5. In case of CNC solutions, if the concentration of background electrolyte is 0.001 M (Figure 5), the reference point (w/o titrant) is within the positive range of proton adsorption values, which indicates an ongoing specific sorption of cations on the surface of a nanocrystal involved in the neutralization of a surface charge. With the increase in the concentration of background electrolyte, as is known from other studies [6], the repulsion between negatively charged particles and the formation of closer-packed agglomerates is found to become less intensive because the surface charge has been partially neutralized by cations. This explains why proton adsorption values in aqueous dispersions of CNCs decrease from 0.08 to 0.006 mmol/g with the increase in the salt concentrations.

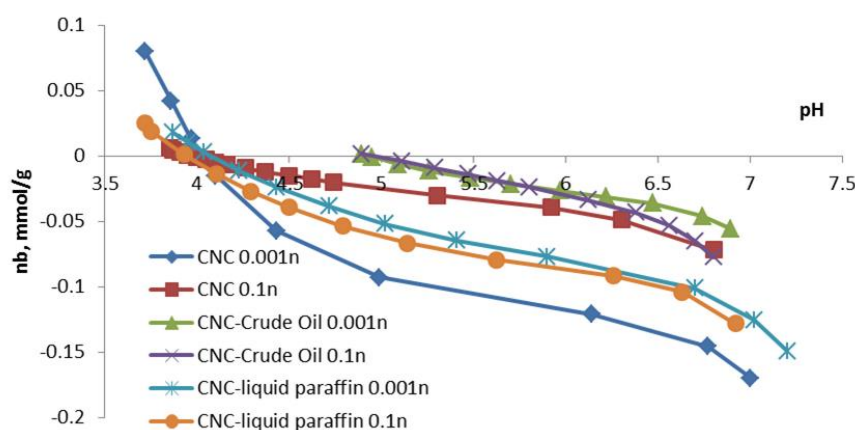


Figure 5. Fluctuation of proton adsorption in co/w and liquid paraffin/water emulsions in relation to pH and concentrations of the background electrolyte (NaCl).

Additional interaction of polar oil molecules with CNCs leads to a considerable shift of the point of zero charge on the cellulose surface (pH_{PZC}) from 3.9 to 4.9 pH units. In the meantime, proton adsorption values almost do not depend on the concentrations of ions of the background electrolyte.

There are two approaches used to interpret the findings of potentiometric titration. The first approach is based on the fact that a charge on the surface of cellulose is a result of the dissociation of surface carboxyl groups [35]. The second approach admits that any group with a dipole moment can be involved in the generation of a negative charge. In the case of native cellulose, it is assumed that oxygen in the hydroxyl group has a certain dipole moment influencing the orientation of water molecules in an interface layer. Influence of surfactants on the structure of the adsorption layer in the system: carboxymethylcellulose/alumina.

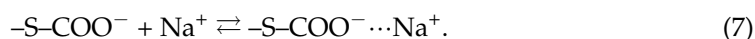
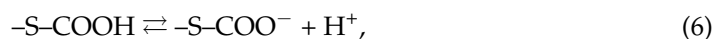
González et al. [22] used the conductometric titration method to define the ionization constants of surface carboxyl groups in nano-fibrillated cellulose with $\text{pK}_a \approx 4$ (1.2 mmol/g), which are fully ionized at $\text{pH} > 6$. For natural cellulose fibers, the presence of two acid–base centers with pK_a 3.5 and 5.7 are shown, and the amount of the second center is lower by an order of magnitude (0.0474 and 0.0049 mmol/g, respectively) [36].

Table 2 demonstrates the calculated dissociation constants for surface groups (pK_i), their concentrations (q_i) and the packing of distributed active acid–base centers on the surface (N_s).

Table 2. Constant values of ionization of surface CNC groups and Pickering emulsions (pK_i), their concentrations (q_i) and packing of active acid–base centers on the surface (N_s).

Sample	C (NaCl), M	pK_i , $\Delta \pm 0.15$	q_i , mmol/g, $\Delta \pm 0.005$	N_s , pcs/nm ² $\Delta \pm 0.003$
CNC	0.001	$\text{pK}_{\text{COOH}} = 3.95$ $\text{pK}_{\text{OH}} = 6.35$	$q_{\text{COOH}} = 0.245$ $q_{\text{OH}} = 0.035$	0.354 0.051
	0.1	$\text{pK}_{\text{COOH}} = 3.95$ $\text{pK}_{\text{OH}} = 6.50$	$q_{\text{COOH}} = 0.060$ $q_{\text{OH}} = 0.030$	0.087 0.043
CNC–liquid paraffin	0.001	$\text{pK}_{\text{COOH}} = 4.85$ $\text{pK}_{\text{OH}} = 6.50$	$q_{\text{COOH}} = 0.095$ $q_{\text{OH}} = 0.030$	0.137 0.043
	0.1	$\text{pK}_{\text{COOH}} = 4.85$ $\text{pK}_{\text{OH}} = 6.50$	$q_{\text{COOH}} = 0.105$ $q_{\text{OH}} = 0.035$	0.152 0.051
CNC–crude oil	0.001	$\text{pK}_{\text{COOH}} = 5.60$ $\text{pK}_{\text{OH}} = 6.65$	$q_{\text{COOH}} = 0.057$ $q_{\text{OH}} = 0.032$	0.082 0.046
	0.1	$\text{pK}_{\text{COOH}} = 5.60$ $\text{pK}_{\text{OH}} = 6.55$	$q_{\text{COOH}} = 0.053$ $q_{\text{OH}} = 0.045$	0.077 0.065

The quantity of acid–base centers with $pK_{\text{COOH}} \approx 4$, in the case of CNC, significantly depends on background electrolyte in the original dispersed medium. With the increase in the concentrations of NaCl, their quantity decreases from 0.245 mmol/g (0.001 M NaCl) to 0.06 mmol/g (0.1 M NaCl). This fact signifies that cations of the background electrolyte participate in the neutralization of a negative charge on the CNC surface ($-S-$), which results from the dissociation of carboxyl groups (as per the first approach). These processes are described in Equations (6) and (7):



With $\text{pH} > 6$, there is a second acid–base center on the surface of the CNC, with $pK \approx 6.4$. It is assumed that it can refer to lactones or residues of lignin molecules [36]. The amount of this center (q_i) is practically independent of the concentration of the background electrolyte. It is assumed that in the case CNC, q_i can be correlated with the deprotonation (Equation (4)) of hydroxyls (pK_{OH}) activated by nearby carboxyl groups, with an increase in pH (according to the second approach):



According to the findings of the TEM and the AFM, the average length of a CNC is 180 ± 40 nm, with a diameter of 6.0 ± 1.0 nm (Figure 1). With the known density of CNCs, i.e., 1.6 g/mL [37,38], and with the quantity (q_i) of acid–base centers per a gram of a sample (Table 2), it will become possible to estimate the distribution rate of active acid–base centers on the cellulose surface (N_S) that are involved in the formation of the Pickering emulsion. Taking into account the significant margin of error when estimating length, the distribution rate of the surface-active acid–base centers was calculated based on the cellulose weight in the sample and the radius of the nanoparticle.

As for emulsions with liquid paraffin, approximately 60% of the surface-active centers become involved in the build of a 2D network at the oil/water interface, causing a shift of the equilibrium constant (Equation (8)) of almost a whole order (from 3.9 to 4.85). The values of pK_{COOH} and their concentrations (q_{COOH}) in such emulsions are basically independent of the concentrations of the background electrolyte. This can be explained by the fact that the cations of the background electrolyte, because they neutralize the repulsion forces between CNCs, manage to achieve a sort of equilibrium with these and thus contribute to better holding the nanoparticles on the oil/water interface. As a result, with the increase in the concentrations of cations, there can be more CNCs on the surface of an emulsion droplet. This is why the titration curves shift towards a more acidic zone, and why the proton adsorption increases in the titration reference point with the increase in salt concentration.

The formation of the emulsion is additionally accompanied by further interactions of the compounds of the polar groups of crude oil with cellulose surface centers. This leads to an additional shifting of the dissociation of carboxyl groups towards $pK_{\text{COOH}} = 5.6$ and to a decrease in the centers involved in this equilibrium from 0.14 (for liquid paraffin) to 0.05 pcs/nm². Moreover, such interactions lead to a higher pK_{OH} , as compared to the emulsions containing liquid paraffin and water dispersion of CNC.

3.3. Rheological Properties of CNC-Stabilized o/w Emulsions

Crude oil emulsions of the water-in-oil type are the ones most commonly used for industrial purposes. They are generated in a natural way during recovery and refining. Crude oil not containing water behaves like Newtonian liquid. Stable oil/water emulsions can be obtained using surfactants of various natures, including solid clay and silicon nanoparticles [39], or, as is demonstrated in this study, using biopolymer nanoparticles.

First of all, we have investigated the effect that the background electrolyte and CNC content have on the viscosity of emulsified crude oil. Low-molecular-weight electrolytes are constant companions of oil emulsions generated in natural offshore areas. This study used emulsions without the NaCl electrolyte, as well as samples with concentrations of 0.01 M, 0.05 M and 0.51 M, typical for the Karskoye sea, which is an area of oil recovery similar to other Arctic offshore areas. CNC-stabilized o/w emulsions of more homogeneous liquid paraffin have been examined as a model compound.

Irrespective of the concentrations of NaCl and CNC, in Pickering emulsions and model systems with liquid paraffin (Figures 6 and S1, respectively), it has been observed that viscosity quickly decreases with an increase in the shift rate and demonstrated shear thinning behaviors, which indicates the gradual destruction of the structure and the bonds between structure elements, as well as solid particles' orientation and the deterioration of aggregates in the area of mechanical impact. The gradual increase in shear stress in the field of high shear rate on the rheological profiles of co/w emulsions and systems with liquid paraffin (Figures 6 and S1C,D) indicates a change in their structure. This includes the possibility of phase boundary distortion, partial deformation and the emulsion droplets' reorientation along the direction of shear. These processes result in a decrease in dynamic viscosity.

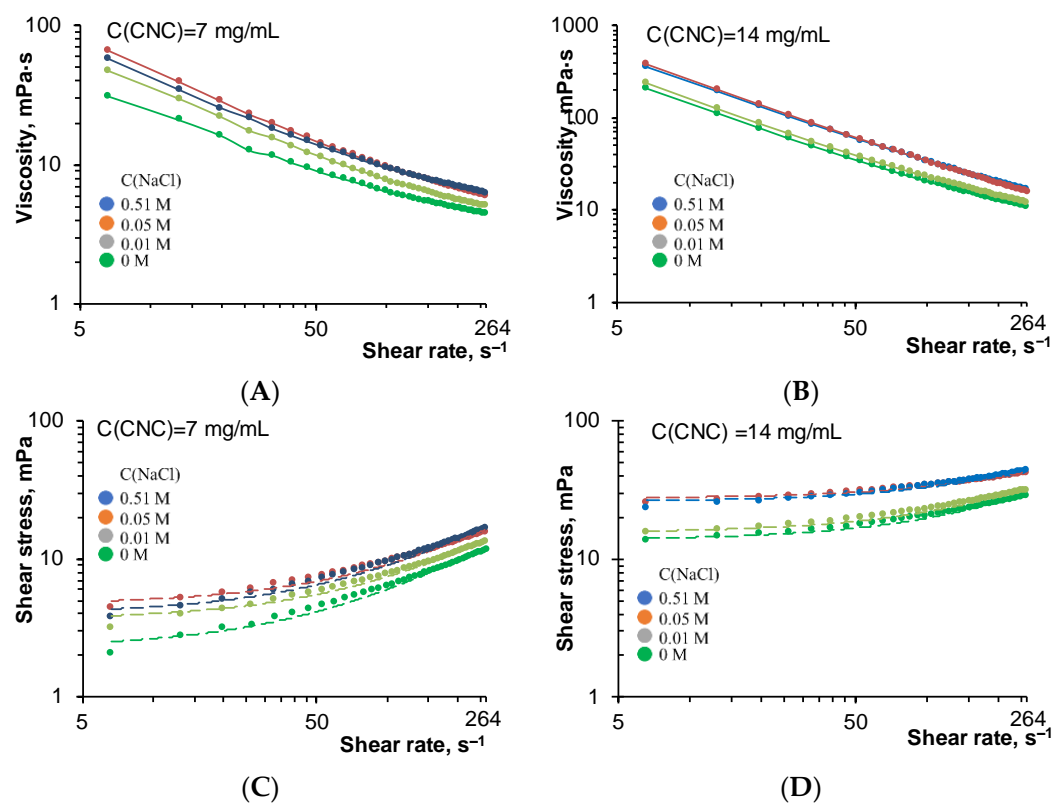


Figure 6. Effect of NaCl addition and CNC concentration on the flow behavior of nanocellulose-stabilized co/w emulsion. (A,B) flow profiles; (C,D) rheological profiles. Experimental data of rheological profiles are presented as the dots. The broken lines are fitting curves.

Approximated graphic dependencies of rheological profiles cross the shear stress axis at the distance of τ_0 from the origin. Thus, there is a yield stress, the exceeding of which leads to viscous flow formation. This demonstrates that the complex structure of systems and the process of structure changes, which is caused by mechanical impact. The obtained graphic dependencies are typical of viscoplastic liquids and pseudoplastic liquids. The dependencies transition to a quasi-Newtonian flow in the high shear rate range, which is commonly seen in o/w emulsions [40,41].

Within the groups of CNC-stabilized emulsions with various contents of stabilizer particles, with the increase in concentrations of NaCl, the viscosity of CNC-stabilized emulsions and of liquid paraffin and crude oil increases. This tendency is clearly seen in the range of C(NaCl) 0–0.05 M (Figure 6A,B) and confirmed by the data in Table S1. The difference between the viscosity of crude oil/w emulsions with an electrolyte concentration of 0.51 M and 0.05 M NaCl is small; in some cases, viscosity of the system which contains larger amount of electrolyte is lower (Table S1). A similar pattern is also observed for the viscosity increment depending on the viscosity of the liquid paraffin o/w emulsion. Special attention is drawn to the increase in the viscosity of CNC-stabilized co/w emulsions under an increase in the stabilizer in the system. This affect is well-known for Pickering emulsions [42]. An increase in CNC concentrations in an emulsified system produces a more intensive effect on the system's viscosity than adding the electrolyte. The increase in viscosity in the case of an increase in the concentrations of the electrolyte and CNCs can be accounted for by more intensive processes of microdroplet flocculation. Adding electrolyte will give rise to the reduction of electrostatic repulsion between negatively charged CNCs [43], and further to the shortening of the distance between particles, followed by an aggregation process. As shown above (Figures 2 and 3), the increase in the mass fraction of CNCs in the system leads to the reduction of the sizes of emulsion droplets due to the formation of a closer-packed structures on the surface of microdroplets. Moreover, as shown in the study by Pal [44], the viscosity of Pickering emulsions depends on the sizes of droplets, i.e., when the same system transforms to smaller microdroplets, an increase in viscosity is observed. Stopping the viscosity increment or a slight decrease in the viscosity of a system with 0.51 M NaCl, in comparison with a 0.05 M NaCl system, indicates that the effect of complete shielding droplets, which have same charge, has already been reached with an electrolyte concentration of 0.05 M. Hence, a further increase in electrolyte concentration up to 0.5 M does not cause structural changes.

Because of the complex structure of the considered emulsions, two mathematical models have used to describe it. It was found that for co/w–CNC systems, the highest correlation coefficient in that range of values for shear rate–shear stress could be obtained using the relatively simple Bingham law. The correlation coefficient (r^2), in this case, ranged from 0.977 to 0.991 (Table 3). Applying another common model, that is the power law model, gives lower correlation coefficients. In the modeling of the rheological behavior of systems with liquid paraffin, the picture is more mixed. The power law model depicts the rheological characteristics of containing 7 mg/mL CNC emulsions more reliably, while for 14 mg/mL systems, higher values of r^2 have been obtained via the Bingham law model (Table S2). That indicates a change of structure formation and flow mechanism under an increase in the stabilizer amount in that type of emulsion.

Table 3. Rheological parameters of CNC-stabilized co/w emulsions at different CNC and salt concentrations.

CNC, mg/mL	C(NaCl), M	Bingham Law				Power Law			
		τ_0 , mPa	μ_p , mPa·s	r^2	μ_a^B (50 s ⁻¹)	K	n	μ_a^{pl} (50 s ⁻¹)	r^2
7	0	2.267	0.038	0.987	0.082	0.697	0.493	0.096	0.985
	0.01	3.625	0.038	0.991	0.111	1.220	0.413	0.123	0.978
	0.05	4.002	0.050	0.987	0.130	1.378	0.432	0.149	0.978
	0.51	4.686	0.044	0.983	0.138	1.827	0.373	0.152	0.974
14	0	13.797	0.061	0.980	0.337	7.527	0.229	0.369	0.948
	0.01	15.581	0.065	0.978	0.377	8.719	0.220	0.412	0.945
	0.05	26.145	0.070	0.978	0.593	15.152	0.181	0.615	0.963
	0.51	27.660	0.058	0.977	0.612	17.595	0.150	0.633	0.960

As can be seen from the provided data, in co/w–CNC systems, values of τ_0 and the apparent viscosity (μ_a) monotonically increase with an increase in electrolyte concentration.

It is known that the higher apparent viscosity, the higher the emulsion stability. The sharp increase (by more than four times) in values of μ_a has also been observed upon transition to a system with a concentration of 14 mg/mL. The observed trends of monotonic increases in μ_a are of the same nature for liquid paraffin o/w–CNC systems (Table S2), which indicates the similar mechanism of stabilization of a given emulsion type. Emulsions of multi-component objects in nature (i.e., crude oil) and liquid paraffin emulsions generally demonstrate a similar rheological behavior. The level of influence of asphaltene, polar groups and other elements of crude oils on the emulsion stability and its rheological properties is generally negated by emulsion droplets' isolation by CNC particles. On the other hand, rheological characteristics analysis indicates differences in the restructuring processes of co/w emulsions and liquid paraffin emulsions.

The findings are consistent with the proposed model of the structure formation of the considered emulsions stabilized by CNC. In the model, the structure is formed by numerous coagulation bonds between cellulose particles on the surface of nearby droplets. Both of these factors lead to the formation of a rigid three-dimensional structure, requiring a high mechanical impact for transition to the viscous flow regime (Bingham plastic model). The strength of the system with C (CNC) = 7 mg/mL is lower, which can be described by the fewer contacts between the less numerous CNC particles. In other words, the formation of a "looser" bond network is occurring.

This research is focused on the initial study of co/w emulsions. A more complete study of the rheology of complex three-phase systems requires a special survey. It should be noted that the Bingham law has been regarded as the most suited and is the most applied for all considered systems. On the other hand, discrepancies between the theoretical and experimental have been observed in some instances; to a greater extent, it has been observed for emulsions with C (CNC) = 7 mg/mL and a low amount of electrolyte. It can be stated that the rheological behavior for those systems in the relatively low mechanical effect range is described by complex models, with three variables. In addition, great scientific and practical interest is being directed at the impact of temperature and counterion on the rheological behavior of that systems.

With regard to biological methods of crude oil destruction, the obtained data allow us to assume that emulsions which were stabilized by a smaller amount of CNCs are more suitable. In this case, they have acceptable stability, small droplet size, looser bond network and lower viscosity, which will contribute to the more intensive penetration of microbial agents and nutrients, as well as to crude oil contact with oil-oxidizing enzymes of yeast and bacteria.

3.4. Biodegradation of CNC-Stabilized o/w Emulsions

A significant limitation of the biological method's application in water treatment is the low bioavailability of crude oil, and in particular, the extremely low solubility in water, which does not allow bacteria to decompose oil. Therefore, the assessment of the effectiveness of biodegradation oil emulsions after the introduction of bacteria–oil destructors is an important issue in obtaining and applying emulsifiers based on biopolymers for the remediation oil spills.

In this section, the influence of natural microorganisms on the biodegradation processes stabilized by cellulose nanocrystals' Pickering emulsions in o/w systems was studied, depending on the ratio of components in the emulsion.

Oil makes a sort of film on the water surface, creating oxygen-deficit conditions. Nanoparticles in the Pickering emulsions can tear this film, with the oil being contained within the interface between the water and the air in the form of separate spherical structures (Figure 7), thus ensuring a partial water/air contact.

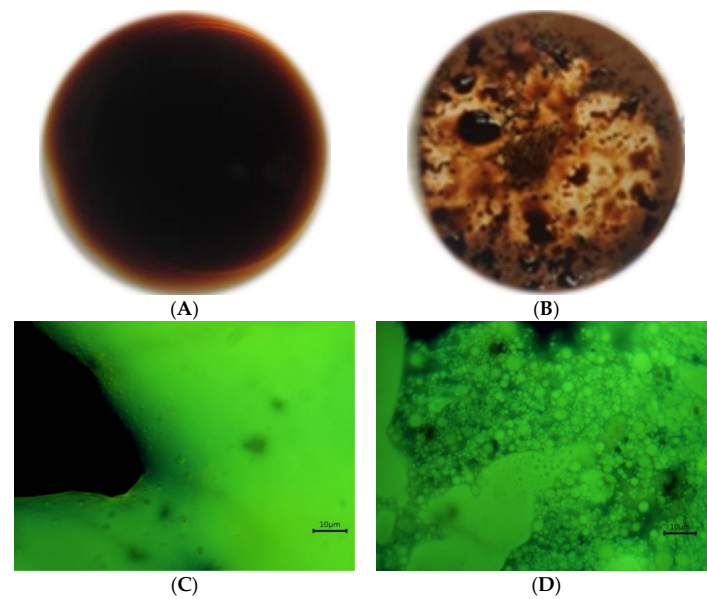


Figure 7. Simulation of oil contamination on water surface and optical microphotograph of oil film fragment collected from the water surface: (A,C) original oil; (B,D) Pickering emulsion in oil/water system.

After 30 days of incubation, total petroleum hydrocarbons content in the control samples showed no major alterations (Table 4). The addition of the inoculum of bacteria enabled a 30–40% decrease in TPH content, which is considered to be a minor-degree intensity of hydrocarbon degradation. The main reason why it is so is the deficit of oxygen required for oil oxidation and the limited contact of bacteria with the oil film at rest (w/o stirring).

Table 4. Total petroleum hydrocarbons (TPH) content in experiments after incubation over 30 days.

Description	Control, Crude Oil	<i>Rhodococcus egui</i>	Emulsion	<i>Rhodococcus egui</i> and Emulsion
Residual content of mineral oils, %	97 ± 20	72 ± 16	74 ± 17	31 ± 8

In the presence of emulsion, the TPH content has become approximately 30% less without adding the inoculum of microorganisms and almost 70% less with the inoculum of bacteria. Direct microscopy showed that bacteria concentrate on the surface of emulsified oil and form a biofilm (Figure 8).

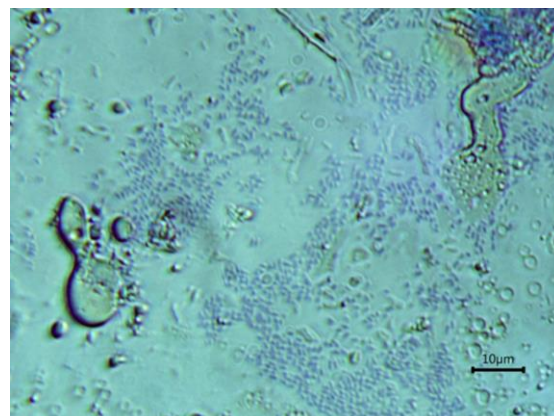


Figure 8. Stock of *Rhodococcus egui* in biofilm (methylene blue dye, direct optical microscopy, ×1500).

Furthermore, the emulsified oil shows the growth of microfungi (Figures 9 and 10), which could have come into contact with the film via the air or could have been directly present in crude oil. Elshafie et al. [45], Al-Hawash et al. [46] and Maddela et al. [47] showed that oil and oil products could serve as a suitable substrate for microfungi species *Aspergillus*, *Penicillium*, *Trichoderma* and *Geomyces*. On the other hand, micromycetes fungi can use nanocellulose particles as a substrate because they are highly cellulolytic. You-Qing et al. [48] and Asemoloye et al. [49] highlighted the synergy of bacteria and fungi during the biodegradation of hydrocarbons. Czemińska et al. [50] and Jain et al. [51] showed that the bacterial biofilm consists of reducing sugars, uronic acids, aminosugars, proteins and sulfates. Potentially, micromycetes can also use an exopolymeric complex of hydrocarbon-oxidizing bacteria as a growth substrate.

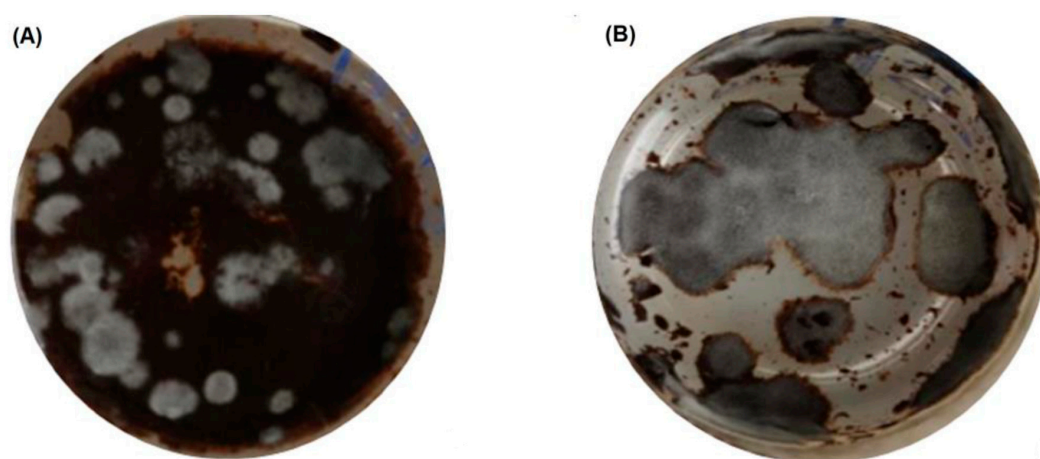


Figure 9. Emulsion of oil covering water surface and damaged by microfungi: (A) oil emulsion without bio-product; (B) with bio-preparation.

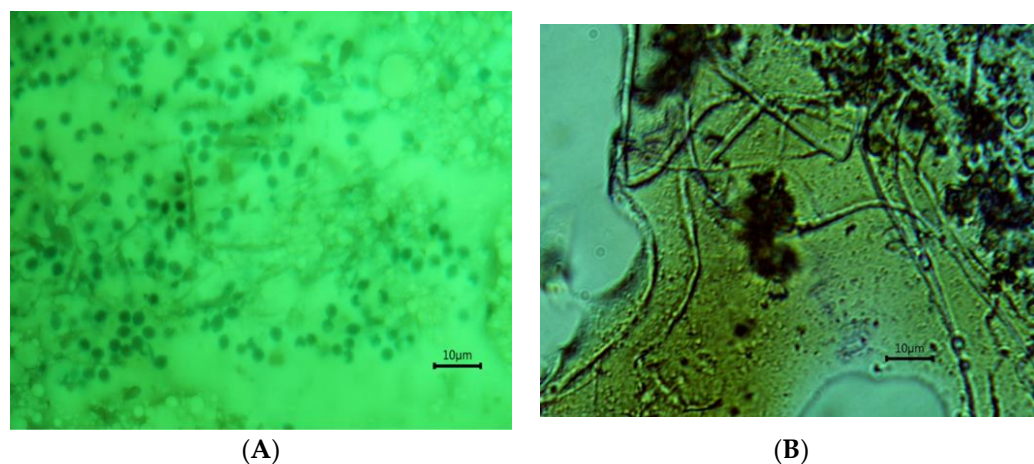


Figure 10. Biofilm damaged by microfungi (fluorescent (A) and direct (B) microscopy, $\times 1500$).

According to the findings of gas chromatography, it was discovered that out of all the oil components, normally structured alkanes are the ones most intensively destroyed (Figure 11). The analysis of chromatographs revealed that the content of n-alkanes up to C_{32} in a control sample was, in fact, reduced by an order, while the content of such branched hydrocarbons as phytane and pristane decreased approximately three times. This means that linear alkanes are rather intensively destroyed by microorganisms from the Pickering emulsion, while iso-alkanes are more resistant to biological oxidation.

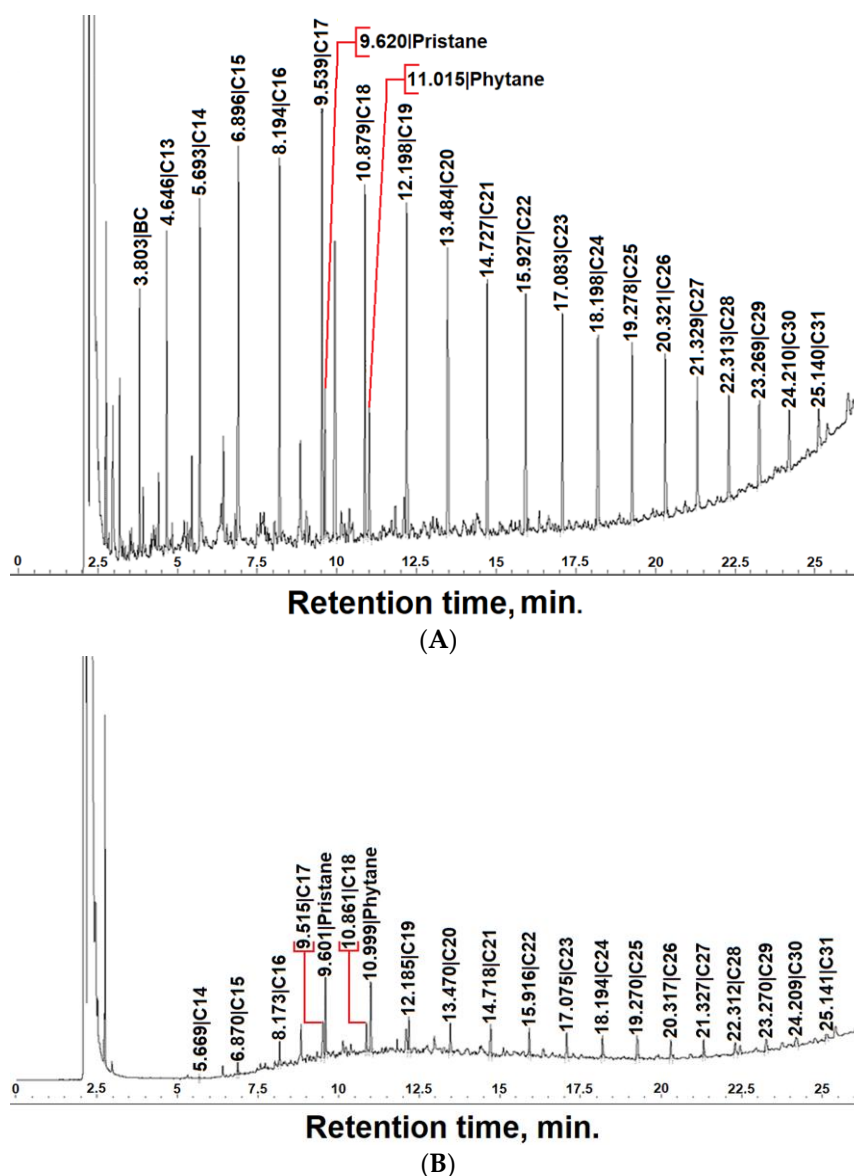


Figure 11. Gas chromatography component analysis of hydrocarbons in oil emulsion before (A) and after (B) treatment with a bio-preparation.

4. Conclusions

The formation of Pickering emulsions in a co/w system stabilized by CNCs with partially acetylated surfaces was studied. In systems containing 3.5 mg/mL of CNCs, when background electrolyte is not available, inverted emulsions are formed in which oil asphaltenes act as surfactants. It was revealed that co/w systems containing larger quantity of CNCs demonstrate the formation of stable emulsions with an average droplet size between 3 μm (CNC content is 7 mg/mL) and 1.5 μm (CNC content is 14 mg/mL). With the rise in the concentration of background electrolyte, the droplet size in co/w emulsions decreases, which is explained by the fact that the cations of the background electrolyte are involved in the neutralization of surface charge.

The rheological behavior of CNC-stabilized o/w emulsions of oil products and crude oil, to a large extent, depends on the colloidal chemical properties of nanocellulose particles. These properties are manifested with greater intensity in a system with a relatively higher CNC content. They also lead to the rapid growth of viscosity with an increase in CNC concentration. Thus, the CNC impact on the rheological characteristics of the emulsion exceeds the influence of the electrolyte. This is caused by a decrease in the size of dispersed

phase elements and the structure formation resulting from the bond network formation between polysaccharide particles on the droplet surface.

Ionization constants for surface acid–base centers (pK_i) and the quantity related to the equilibrium of these centers (q_i) were determined via potentiometric titration. In cases of nanocrystal derivatives of cellulose, there may be two mechanisms of the emergence of a negative surface charge depending on pH: first, as a result of the dissociation of surface carboxyl groups ($pK_{COOH} \approx 4$); second, due to the deprotonation of hydroxyl groups ($pK_{OH} \approx 6.5$). The formation of emulsion is accompanied by a further interaction of the compounds of polar groups of crude oil with the cellulose surface centers. This ends in the further shifting of the dissociation of carboxyl groups towards $pK_{COOH} = 5.6$ and in a decrease in the centers involved in the specified equilibrium from 0.14 (for liquid paraffin) to 0.05 pcs/nm². Moreover, such interactions lead to a higher pK_{OH} compared to the emulsions containing liquid paraffin and water dispersion of CNCs.

The use of oil and CNCs as a basis for the formation of Pickering emulsions ensures the preservation of water/air contact at the interface, encouraging a more effective oxidation of oil by the bacteria, *Rhodococcus egvi*, in the aerobic environment provided there are mineral salts of nitrogen, potassium and phosphorous in the environment. The results obtained serve as a scientific basis for the development of technologies for the disposal of oil spills on water surfaces.

Supplementary Materials: The following supporting information can be downloaded at <https://www.mdpi.com/article/10.3390/polysaccharides4040024/s1>, Figure S1: Effect of NaCl addition and CNC concentration on the flow behavior of nanocellulose stabilized liquid paraffin o/w emulsion. (a,b)—flow profiles; (c,d)—rheological profiles; Table S1: Dynamic viscosity of CNC-stabilized o/w emulsions at different CNC and salt concentrations, mPa·s; Table S2: Rheological parameters of CNC-stabilized liquid paraffin o/w emulsion at different CNC and salt concentrations.

Author Contributions: Conceptualization, P.S. and M.T.; methodology, P.S. and M.T.; validation, E.U.; formal analysis, P.S., P.L., M.T., Y.D., V.M., D.T. and I.V.; investigation, P.S., P.L., M.T., Y.D., V.M., D.T., I.V., M.M. and N.U.; resources, M.M. and E.U.; writing—original draft preparation, P.S., P.L., M.T., D.T. and I.V.; writing—review and editing, P.S. and E.U.; supervision, E.U. All authors have read and agreed to the published version of the manuscript.

Funding: This study was supported by a Grant of the Russian Science Foundation No. 22-23-00271, <https://rscf.ru/en/project/22-23-00271/> (accessed on 26 October 2023).

Institutional Review Board Statement: Not applicable.

Data Availability Statement: Data will be made available on request.

Acknowledgments: Investigations were partially carried out using the equipment of the “Khimiya” Common Use Centre (Institute of Chemistry, FRC Komi SC UB RAS). Studying the biodegradation of crude oil emulsions was carried out at the expense of state tasks of the Institute of Biology of Komi Scientific Centre of the Ural Branch of the Russian Academy of Sciences (No. 122040600019-1).

Conflicts of Interest: The authors declare no conflict of interest.

References

1. Low, L.E.; Siva, S.P.; Ho, Y.K.; Chan, E.S.; Tey, B.T. Recent advances of characterization techniques for the formation, physical properties and stability of Pickering emulsion. *Adv. Colloid Interface Sci.* **2020**, *277*, 102117. [[CrossRef](#)] [[PubMed](#)]
2. Binks, B.P.; Lumsdon, S.O. Pickering emulsions stabilized by monodisperse latex particles: Effects of particle size. *Langmuir* **2001**, *17*, 4540–4547. [[CrossRef](#)]
3. Tsugita, A.; Takemoto, S.; Mori, K.; Yoneya, T.; Otani, Y. Studies on OW emulsions stabilized with insoluble montmorillonite-organic complexes. *J. Colloid Interface Sci.* **1983**, *95*, 551–560. [[CrossRef](#)]
4. Avazpour, R.; Latifi, M.; Chaouki, J.; Fradette, L. Physical beneficiation of rare earth-bearing ores by Pickering emulsification. *Miner. Eng.* **2019**, *144*, 106034. [[CrossRef](#)]
5. Radnia, H.; Nazar, A.R.S.; Rashidi, A. Effect of asphaltene on the emulsions stabilized by graphene oxide: A potential application of graphene oxide in enhanced oil recovery. *J. Pet. Sci. Eng.* **2019**, *175*, 868–880. [[CrossRef](#)]
6. Kalashnikova, I.; Bizot, H.; Cathala, B.; Capron, I. New Pickering emulsions stabilized by bacterial cellulose nanocrystals. *Langmuir* **2011**, *27*, 7471–7479. [[CrossRef](#)]

7. Perrin, E.; Bizot, H.; Cathala, B.; Capron, I. Chitin nanocrystals for Pickering high internal phase emulsions. *Biomacromolecules* **2014**, *15*, 3766–3771. [[CrossRef](#)]
8. Trache, D.; Tarchoun, A.F.; Derradji, M.; Hamidon, T.S.; Masruchin, N.; Brosse, N.; Hussin, M.H. Nanocellulose: From Fundamentals to Advanced Applications. *Front. Chem.* **2020**, *8*, 392. [[CrossRef](#)]
9. Kalashnikova, I.; Bizot, H.; Cathala, B.; Capron, I. Modulation of cellulose nanocrystals amphiphilic properties to stabilize oil/water interface. *Biomacromolecules* **2012**, *13*, 267–275. [[CrossRef](#)]
10. Kalashnikova, I.; Bizot, H.; Bertoncini, P.; Cathala, B.; Capron, I. Cellulosic nanorods of various aspect ratios for oil in water Pickering emulsions. *Soft. Matter.* **2013**, *9*, 952–959. [[CrossRef](#)]
11. Bai, L.; Greca, L.G.; Xiang, W.; Lehtonen, J.; Huan, S.; Nugroho, R.W.N.; Tardy, B.L.; Rojas, O.J. Adsorption and assembly of cellulosic and lignin colloids at oil/water interfaces. *Langmuir* **2018**, *35*, 571–588. [[CrossRef](#)] [[PubMed](#)]
12. Cerbelaud, M.; Aimable, A.; Videcoq, A. Role of electrostatic interactions in oil-in-water emulsions stabilized by heteroaggregation: An experimental and simulation study. *Langmuir* **2018**, *34*, 15795–15803. [[CrossRef](#)]
13. Hu, Z.; Ballinger, S.; Pelton, R.; Cranston, E.D. Surfactant-enhanced cellulose nanocrystal Pickering emulsions. *J. Colloid Interface Sci.* **2015**, *439*, 139–148. [[CrossRef](#)] [[PubMed](#)]
14. Torlopov, M.A.; Martakov, I.S.; Mikhaylov, V.I.; Golubev, Y.A.; Sitnikov, P.A.; Udoratina, E.V. A Fenton-like system (Cu (II)/H₂O₂) for the preparation of cellulose nanocrystals with a slightly modified surface. *Ind. Eng. Chem.* **2019**, *58*, 20282–20290. [[CrossRef](#)]
15. Capron, I.; Cathala, B. Surfactant-free high internal phase emulsions stabilized by cellulose nanocrystals. *Biomacromolecules* **2013**, *14*, 291–296. [[CrossRef](#)] [[PubMed](#)]
16. Li, C.; Zhang, H.; Long, Y.; Ni, Y. Preparation of cellulose nanocrystals from asparagus (*Asparagus officinalis* L.) and their applications to palm oil/water Pickering emulsion. *Carbohydr. Polym.* **2016**, *151*, 1–8. [[CrossRef](#)]
17. Chen, Q.; Liu, Q. Bitumen coating on oil sands clay minerals: A Review. *Energy Fuels* **2019**, *33*, 5933–5943. [[CrossRef](#)]
18. Alves, D.R.; Carneiro, J.S.A.; Oliveira, I.F.; Façanha, F., Jr.; Santos, A.F.; Dariva, C.; Franceschi, E.; Fortune, M. Influence of the salinity on the interfacial properties of a Brazilian crude oil–brine systems. *Fuel* **2014**, *118*, 21–26. [[CrossRef](#)]
19. Nour, A.H.; Yunus, R.M.; Anwaruddin, H. Water-in-crude oil emulsions: Its stabilization and demulsification. *J. Appl. Sci.* **2007**, *7*, 3512–3517. [[CrossRef](#)]
20. Anaclet, P.; Depardieu, M.; Laurichesse, E.; Julien, V.; Hung, Y.; Schmitt, V.; Backov, R. Bitumen@SiO₂ core-shell particles green synthesis towards flowable powdered bitumen and their binder applications. *Colloids Surf. A* **2019**, *570*, 531–543. [[CrossRef](#)]
21. Ortiz, D.P.; Baydak, E.N.; Yarranton, H.W. Effect of surfactants on interfacial films and stability of water-in-oil emulsions stabilized by asphaltenes. *J. Colloid Interface Sci.* **2010**, *351*, 542–555. [[CrossRef](#)] [[PubMed](#)]
22. González, M.M.; Blanco-Tirado, C.C.; Combariza, M.Y. Nanocellulose as an inhibitor of water-in-crude oil emulsion formation. *Fuel* **2020**, *264*, 116830. [[CrossRef](#)]
23. Löser, C.; Seidel, H.; Zehnsdorf, A.; Stottmeister, U. Microbial degradation of hydrocarbons in soil during aerobic/anaerobic changes and under purely aerobic conditions. *Appl. Microbiol. Biotechnol.* **1998**, *49*, 631–636. [[CrossRef](#)]
24. Wu, M.; Dick, W.A.; Li, W.; Wang, X.; Yang, Q.; Wang, T.; Xu, L.; Zhang, M.; Chen, L. Bioaugmentation and biostimulation of hydrocarbon degradation and the microbial community in a petroleum-contaminated soil. *Int. Biodeterior. Biodegrad.* **2016**, *107*, 158–164. [[CrossRef](#)]
25. Beškoski, V.P.; Gojgić-Cvijović, G.; Milić, J.; Ilić, M.; Miletić, S.; Šolević, T.; Vrvić, M.M. Ex situ bioremediation of a soil contaminated by mazut (heavy residual fuel oil)—A field experiment. *Chemosphere* **2011**, *83*, 34–40. [[CrossRef](#)]
26. Birch, H.; Hammershøj, R.; Comber, M.; Mayer, P. Biodegradation of hydrocarbon mixtures in surface waters at environmentally relevant levels—Effect of inoculum origin on kinetics and sequence of degradation. *Chemosphere* **2017**, *184*, 400–407. [[CrossRef](#)]
27. Polyak, Y.M.; Bakina, L.G.; Chugunova, M.V.; Mayachkina, N.V.; Gerasimov, A.O.; Bure, V.M. Effect of remediation strategies on biological activity of oil-contaminated soil—A field study. *Int. Biodeterior. Biodegrad.* **2018**, *126*, 57–68. [[CrossRef](#)]
28. Ahearn, D.G.; Meyers, S.P. *The Microbial Degradation of Oil Pollutants: Workshop Held at Georgia State University, Atlanta, December, 1972*; Ahearn, D.G., Meyers, S.P., Eds.; Center for Wetland Resources, Louisiana State University: Baton Rouge, LA, USA, 1973; Volume 73, No. 1.
29. Parajuli, S.; Alazzam, O.; Wang, M.; Mota, L.C.; Adhikari, S.; Wicks, D.; Ureña-Benavides, E.E. Surface properties of cellulose nanocrystal stabilized crude oil emulsions and their effect on petroleum biodegradation. *Colloids Surf. A* **2020**, *596*, 124705. [[CrossRef](#)]
30. Torlopov, M.A.; Mikhaylov, V.I.; Udoratina, E.V.; Aleshina, L.A.; Prusskii, A.I.; Tsvetkov, N.V.; Krivoshapkin, P.V. Cellulose nanocrystals with different length-to-diameter ratios extracted from various plants using novel system acetic acid/phosphotungstic acid/octanol-1. *Cellulose* **2018**, *25*, 1031–1046. [[CrossRef](#)]
31. Ionescu, C.M.; Birs, I.R.; Copot, D.; Muresan, C.I.; Caponetto, R. Mathematical modelling with experimental validation of viscoelastic properties in non-Newtonian fluids. *Phil. Trans. R. Soc. A* **2020**, *378*, 20190284. [[CrossRef](#)]
32. Abbastabar, B.; Azizi, M.H.; Adnani, A.; Abbasi, S. Determining and modeling rheological characteristics of quince seed gum. *Food Hydrocol.* **2015**, *43*, 259–264. [[CrossRef](#)]
33. Ryazanov, M.A.; Dudkin, B.N. Acid-base properties of the surface of the α -Al₂O₃ suspension. *Russ. J. Phys. Chem. A* **2009**, *83*, 2318–2321. [[CrossRef](#)]

34. Tarabukin, D.V.; Torlopov, M.A.; Shchemelinina, T.N.; Anchugova, E.M.; Shergina, N.N.; Istomina, E.I.; Belyy, V.A. Biosorbents based on esterified starch carrying immobilized oil-degrading microorganisms. *J. Biotechnol.* **2017**, *260*, 31–37. [[CrossRef](#)] [[PubMed](#)]
35. Van der Vegte, E.W.; Hadziioannou, G. Acid– base properties and the chemical imaging of surface-bound functional groups studied with scanning force microscopy. *J. Phys. Chem. B* **1997**, *101*, 9563–9569. [[CrossRef](#)]
36. Fras, L.; Laine, J.; Stenius, P.; Stana-Kleinschek, K.; Ribitsch, V.; Doleček, V. Determination of dissociable groups in natural and regenerated cellulose fibers by different titration methods. *J. Appl. Polym. Sci.* **2004**, *92*, 3186–3195. [[CrossRef](#)]
37. Thomas, B.; Raj, M.C.; Athira, B.K.; Rubiyah, H.M.; Joy, J.; Moores, A.; Drisko, G.L.; Sanchez, C. Nanocellulose, a versatile green platform: From biosources to materials and their applications. *Chem. Rev.* **2018**, *118*, 11575–11625. [[CrossRef](#)]
38. Abitbol, T.; Kam, D.; Levi-Kalishman, Y.; Gray, D.G.; Shoseyov, O. Surface charge influence on the phase separation and viscosity of cellulose nanocrystals. *Langmuir* **2018**, *34*, 3925–3933. [[CrossRef](#)]
39. Simon, S.; Theiler, S.; Knudsen, A.; Øye, G.; Sjöblom, J. Rheological properties of particle-stabilized emulsions. *J. Dispers. Sci. Technol.* **2010**, *31*, 632–640. [[CrossRef](#)]
40. Frigaard, I.A.; Paso, K.G.; de Souza Mendes, P.R. Bingham’s model in the oil and gas industry. *Rheol. Acta* **2017**, *56*, 259–282. [[CrossRef](#)]
41. Ariffin, T.S.T.; Yahya, E.; Husin, H. The Rheology of light crude oil and water-in-oil-emulsion. *Procedia Eng.* **2016**, *148*, 149–1155. [[CrossRef](#)]
42. Ghasemi, R.; Fazlali, A.; Mohammadi, A.H. Effects of TiO₂ nanoparticles and oleic acid surfactant on the rheological behavior of engine lubricant oil. *J. Mol. Liq.* **2018**, *268*, 925–930. [[CrossRef](#)]
43. Mikhailov, V.I.; Torlopov, M.A.; Martakov, I.S.; Krivoschapkin, P.V. Stability of nanocrystalline cellulose in aqueous KCl solutions. *Colloid. J.* **2017**, *79*, 226–233. [[CrossRef](#)]
44. Pal, R. A simple model for the viscosity of Pickering emulsions. *Fluids* **2018**, *3*, 2. [[CrossRef](#)]
45. Elshafie, A.; AlKindi, A.Y.; Al-Busaidi, S.; Bakheit, C.; Albahry, S.N. Biodegradation of crude oil and n-alkanes by fungi isolated from Oman. *Mar. Pollut. Bull.* **2007**, *54*, 1692–1696. [[CrossRef](#)] [[PubMed](#)]
46. Al-Hawash, A.B.; Alkooranee, J.T.; Abbood, H.A.; Zhang, J.; Sun, J.; Zhang, X.; Ma, F. Isolation and characterization of two crude oil-degrading fungi strains from Rumaila oil field, Iraq. *Biotechnol. Rep.* **2018**, *17*, 104–109. [[CrossRef](#)]
47. Maddela, N.R.; Burgos, R.; Kadiyala, V.; Carrion, A.R.; Bangeppagari, M. Removal of petroleum hydrocarbons from crude oil in solid and slurry phase by mixed soil microorganisms isolated from Ecuadorian oil fields. *Int. Biodeterior. Biodegrad.* **2016**, *108*, 85–90. [[CrossRef](#)]
48. You-Qing, L.I.; Hong-Fang, L.I.U.; Zhen-Le, T.; Li-Hua, Z.H.U.; Ying-Hui, W.U.; He-Qing, T. Diesel pollution biodegradation: Synergetic effect of *Mycobacterium* and filamentous fungi. *Biomed. Environ. Sci.* **2008**, *21*, 181–187. [[CrossRef](#)]
49. Asemoloye, M.D.; Ahmad, R.; Jonathan, S.G. Synergistic action of rhizospheric fungi with *Megathyrus maximus* root speeds up hydrocarbon degradation kinetics in oil polluted soil. *Chemosphere* **2017**, *187*, 1–10. [[CrossRef](#)]
50. Czemińska, M.; Szcześ, A.; Pawlik, A.; Wiater, A.; Jarosz-Wilkolazka, A. Production and characterisation of exopolymer from *Rhodococcus opacus*. *Biochem. Eng. J.* **2016**, *112*, 1110–1116. [[CrossRef](#)]
51. Jain, R.M.; Mody, K.; Mishra, A.; Jha, B. Physicochemical characterization of biosurfactant and its potential to remove oil from soil and cotton cloth. *Carbohydr. Polym.* **2012**, *89*, 143–152. [[CrossRef](#)]

Disclaimer/Publisher’s Note: The statements, opinions and data contained in all publications are solely those of the individual author(s) and contributor(s) and not of MDPI and/or the editor(s). MDPI and/or the editor(s) disclaim responsibility for any injury to people or property resulting from any ideas, methods, instructions or products referred to in the content.